

FINAL SCIENTIFIC REPORT

OTKA-NNF 78918

“Molecular diversity and plasticity of endocannabinoid signaling at cortical synapses”

Publications supported by the OTKA-NNF 78918 grant

Published

Ludányi A, Hu SS-J, Yamazaki M, Tanimura A, Piomelli D, Watanabe M, Kano M, Sakimura K, Maglóczy Z, Mackie K, Freund TF és Katona I (2011) Complementary synaptic distribution of enzymes responsible for synthesis and inactivation of the endocannabinoid 2-arachidonoylglycerol in the human hippocampus. *Neuroscience* 174: 50-63.

Submitted

Dudok B, Bokor H, Urbán GM, Yamazaki M, Tanimura A, Kano M, Sakimura K, Zimmer A, Watanabe M, Mackie K, Freund TF, Acsády L and Katona I (2011) Synapse-specific heterogeneity of endocannabinoid signaling in the somatosensory cortex. *Submitted to Cerebral Cortex*.

In preparation

Sepers M, Jung KM, Henstridge CM, Lassalle O, Neuhofer D, Ginger M, Frick A, Mackie K, Katona I, Piomelli D. and Manzoni O.J. (2011) Uncoupling of the endocannabinoid signalosome in a mouse model of fragile X. *Submission to Nature Neuroscience is planned for April, 2011.*

Publicity measures, participation at conferences

Posters

Aniko Ludanyi, Zsafia Magloczky, Ken Mackie, Tamas F Freund, Istvan Katona (2010) Synaptic localization of the enzymatic machinery responsible for 2-arachidonoylglycerol synthesis and degradation in the human hippocampus. IBRO International Workshop 2010

Barna Dudok, Tamás F Freund, István Katona (2010) Development of perisomatic innervation of pyramidal neurons arising from CB1- and parvalbumin-positive basket cells in the mouse visual cortex. Forum of European Neuroscience 2010, (Abstract 191.10.)

Ludanyi A., Magloczky Z., Mackie K., Hu S. S., Freund T. F., Katona I. (2010) Synaptic localization of enzymes responsible for the synthesis and degradation of the endocannabinoid 2-arachidonoylglycerol in human hippocampus. Forum of European Neuroscience 2010, (Abstract 163.23.)

Lectures

Katona I, Dudok B, Ludányi A, Nyilas A, Urbán GM, Freund TF, Watanabe M, Mackie K (2010) Az endokannabinoid jelpályák molekuláris sokfélesége és szerepe a glutamaterg szinapszisok működésében. Magyar Élettani Társaság LXXIV. Vándorgyűlése 2010.

Katona I. (2010) Compartmentalized distribution and functional segregation of distinct endocannabinoid signaling pathways at glutamatergic synapses of the central nervous system. FENS Forum 2010, 030.4.

Summary of the scientific achievements

Specific aim 1

Endocannabinoids (eCBs) are retrograde lipid messengers regulating short- and long-term forms of synaptic plasticity throughout the nervous system (Chevalere et al., 2006). The substantial role of the eCB system in neuronal function is well supported by its involvement in various diseases of the CNS (Pacher et al., 2006). Several different mechanisms of eCB-dependent synaptic plasticity have been described in different layers of the neocortex, including stimulation-induced, pairing-induced, and spike-timing dependent depression (Birtoli and Ulrich, 2004; Nevian and Sakmann, 2006; Crozier et al., 2007). The exact molecular composition of synaptic eCB signaling is well described in some brain regions, e.g. the hippocampus, where activation of metabotropic glutamate receptors leads to the postsynaptic production of 2-arachidonoylglycerol (2-AG) by diacylglycerol

lipase (DGL)- α , and finally to the engagement of presynaptic type 1 cannabinoid receptors (CB₁), inhibiting neurotransmitter release (Katona and Freund, 2008). Striking evidence has shown that enzymes and receptors of the delicate molecular machinery for eCB-mediated depression is required for the experience-dependent maturation of the developing somatosensory cortex (Hannan et al., 2001; Deshmukh et al., 2007; Wijetunge et al., 2008). However, in the neocortex, the molecular source of 2-AG release has not been assessed, and anatomical studies could not detect CB₁ on glutamatergic axon terminals. Moreover, our knowledge was very limited on the molecular background of the massive laminar- and pathway-specific differences in the inducibility of various forms of eCB-mediated depression. Thus, the aim of this project was to decipher the precise localization of the molecular source and target of eCB signaling, DGL- α and CB₁, respectively, in various somatosensory cortical synapses.

Objective 1

To assess the cellular expression pattern of DGL- α , we carried out in situ hybridization (ISH) with digoxigenin-labeled riboprobes against a 1169 base long sequence of the DGL- α mRNA (Fig. 1). The staining revealed expression in cells throughout the forebrain, with moderate to high expression levels in the hippocampus, neocortex, thalamus, striatum and amygdala. In the somatosensory cortex, all pyramidal cell layers were labeled, with the highest intensity in layers II-III and V. These findings indicate that the vast number of principal cells express DGL- α in the somatosensory cortex, and overall in the forebrain. We also noted some sparsely located, weakly labeled cells in layer I of the neocortex, in which principal cells are absent indicating that DGL- α is also expressed by some interneuron types. We validated the specificity of the staining process using sense riboprobes.



Objective 2

We have elucidated the subcellular localization of DGL- α in the somatosensory cortex using an antibody generated against an intracellular loop of this serine hydrolase (DGL- α INT, described by Katona et al., 2006). The staining resulted in a dense punctate pattern in the neuropil of all layers, strongest in layers I-IV, while cell bodies and dendritic segments of neurons remained immunonegative (Fig 2-3). Electron microscopic analysis of the stainings from 3 animals revealed that DGL- α is present postsynaptically in the majority ($65.1 \pm 1.6\%$) of glutamatergic synapses, and, although at a substantially weaker level, in some ($9.3 \pm 1.3\%$) GABAergic synapses as well (Fig 3). Using immunogold labeling, we have shown that the enzyme is precisely targeted to the plasma membrane of dendritic spines, at the close vicinity of synapses, but very rarely inside the postsynaptic density itself. Unfortunately, our collaborator (Prof. Andreas Zimmer) could not accomplish the generation of the proposed DGL- α knockout mice to date. However, we could obtain fixed brain samples of wild-type and DGL- α knockout animals (littermates) from Prof. Masanobu Kano, University of Tokyo. Immunostaining for DGL- α in these samples confirmed the specificity of the antibody we used in these studies (Figure 2).

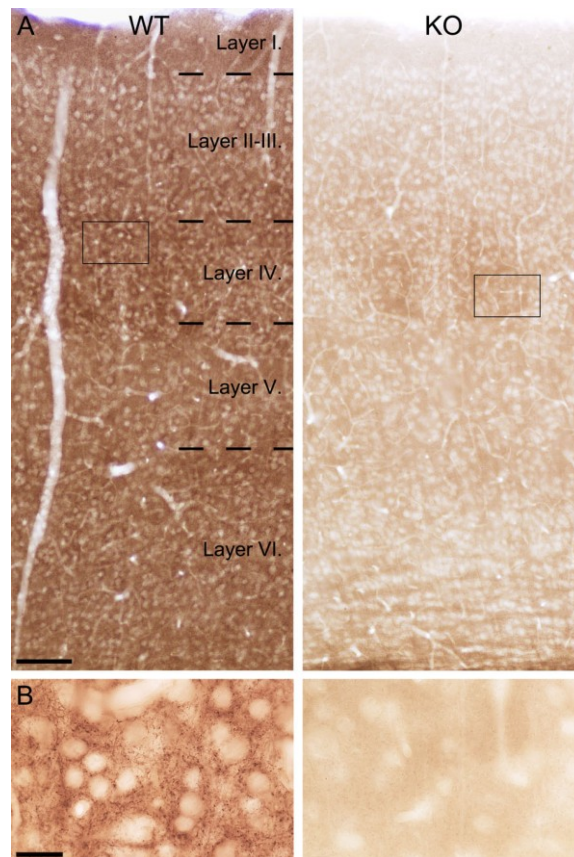


Figure 2. To confirm the specificity of our antibody and staining process, we performed DGL- α immunostaining on sections from wild-type (WT), and DGL- α knockout littermates (KO). The very low intensity of staining, and the lack of the characteristic punctate pattern in the KO sections indicates the specificity of the labeling. Scale bars: 100 μ m for (A), 20 μ m for (B).

We attempted to reveal possible laminar- or pathway-specific variations in the molecular composition of the endocannabinoid system. First, we have utilized quantitative electron microscopic analysis of different neocortical layers to detect any difference in the presence of DGL- α at glutamatergic synapses. We have compared layers I, II-III and IV, all of which receive excitatory input from different sources, and express different forms of eCB-dependent plasticity. However, analysis of 300 spines of each layers (utilizing different antibody dilutions to avoid saturation of the sensitivity of the staining) detected no significant laminar differences in the ratio of immunoreactive synapses ($p > 0.4$ with all dilutions, Kruskal-Wallis test, $n=3$ animals).

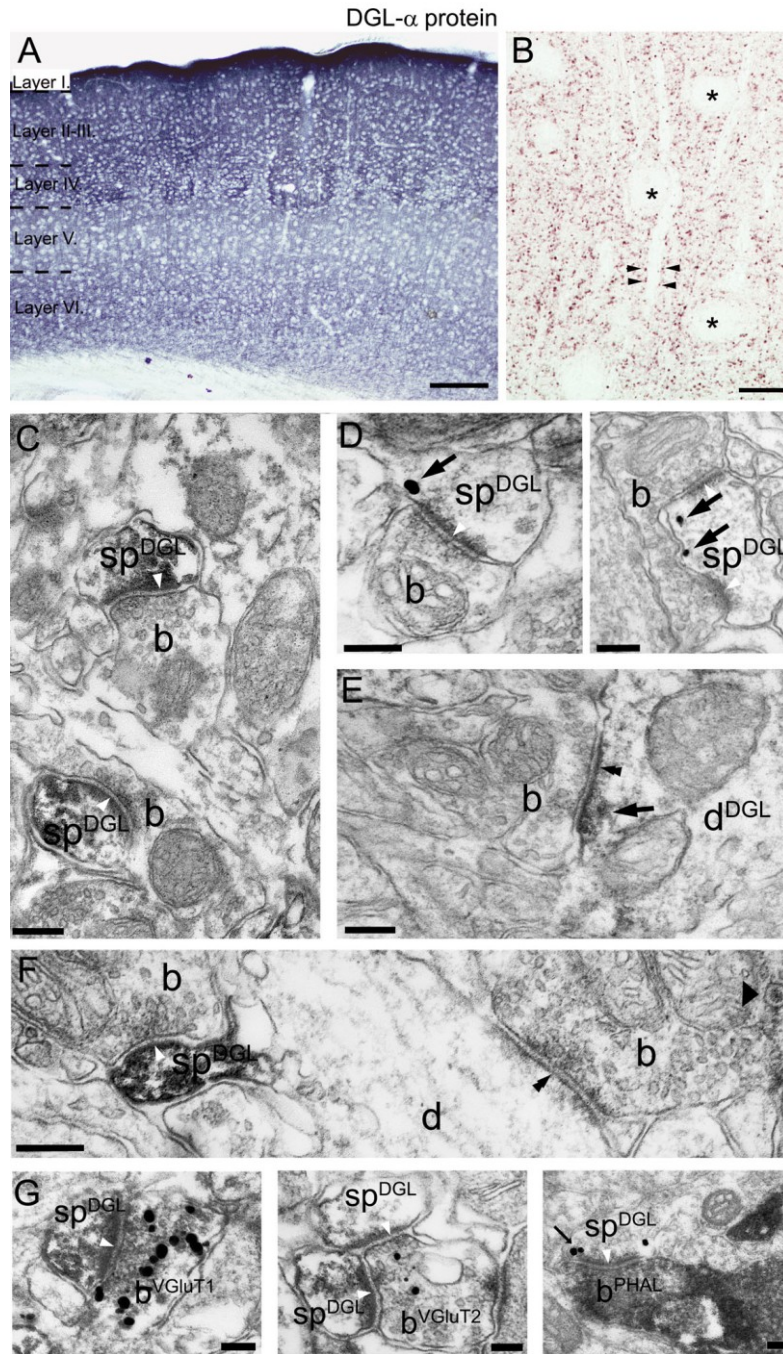


Figure 3. DGL- α is located postsynaptically at neocortical synapses. At the light microscopic level, DGL- α can be detected in all layers of the neocortex, with the highest intensities in layers I-IV, as revealed by peroxidase-based immunohistochemistry (A). At high-power micrographs of semithin sections (B), a punctate staining pattern can be observed in the neuropil, avoiding somata (asterisks) and dendritic shafts (arrowheads). At the electron microscopic level (C), DGL- α immunoreactivity could be observed in dendritic spines (sp), near asymmetric synapses (white arrowheads) raised by glutamatergic boutons (b). Immunogold labeling (D) revealed that the enzyme is confined to the postsynaptic plasma membrane, near the edge of the postsynaptic density. (E) While low levels of immunoreactivity (arrow) associated to symmetric synapses (double arrowheads) raised by GABAergic boutons can be detected in dendritic shafts (d), the striking accumulation of labeling in dendritic spines compared to shafts (F) indicates substantially higher enzyme levels at glutamatergic synapses. (G) Combined immunogold-immunoperoxidase stainings prove that DGL- α is present both at intracortical synapses (identified based on VGLuT1 immunoreactivity), and at thalamocortical synapses (identified by either VGLuT2 immunoreactivity, or the presence of anterograde tracer injected into the thalamus). Scale bars: 200 μ m for (A), 20 μ m for (B), 200 nm for (C-F), 100 nm for (G).

Next, we studied the precise localization of the enzymes DGL- α and monoacylglycerol lipase (MGL) performing the synthesis and degradation, respectively, of the most abundant endocannabinoid, 2-AG in the human hippocampus (Ludányi et al., 2011). In the human hippocampus, immunoreactivity for DGL- α appeared to correspond with the distinct incoming glutamatergic pathways, and was particularly robust in the stratum radiatum (Figure 4). At high magnification, a dense granular pattern corresponding to DGL- α immunoreactivity was visible, which was located on the surface of immunonegative dendrites (Fig.4A). MGL immunoreactivity proved to be very similar to that of DGL- α following the different layers of the human hippocampus. The pattern of immunostaining was also very similar at high magnification: the main immunonegative apical dendrites were covered with a dense punctate immunopositive signal (Fig. 4B). Further electron microscopic studies revealed that DGL- α -immunoreactivity is present exclusively in the postsynaptic dendritic spine heads contacting asymmetric synapses (Fig. 4C). Conversely, MGL immunostaining was found presynaptically in the axon terminals of these excitatory synapses (Fig. 4D). Our anatomical findings show that the main enzymes responsible for 2-AG metabolism have the same subcellular localization in the mouse and human hippocampus suggesting an evolutionarily conserved role of 2-AG in retrograde signaling. As the components of the endocannabinoid system are potential molecular targets in numerous neurological diseases, their conserved localization may be of great importance in future drug discovery.

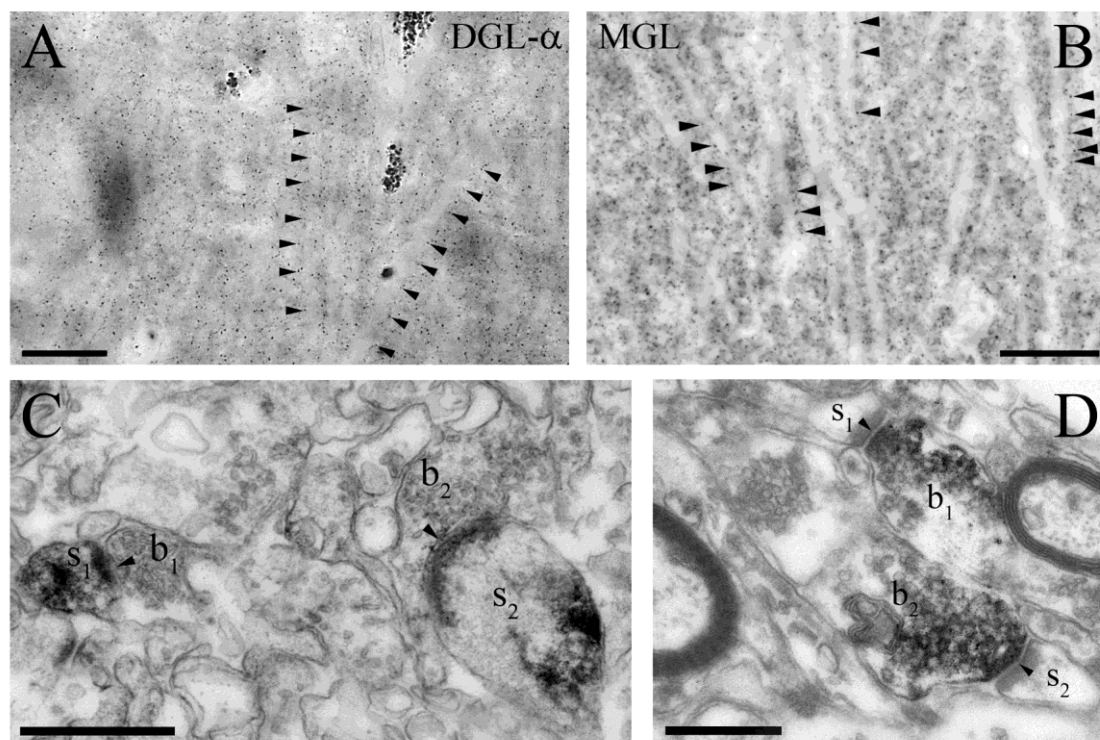


Figure 4. Light- and electron microscopic distribution of enzymes responsible for 2-AG metabolism in the human hippocampus. DGL- α (A) and MGL (B) immunostaining appeared as a dense punctate pattern (arrowheads) in the radiatum layer of the human hippocampus, and highlighted the immunonegative apical dendrites of the pyramidal cells. At the electron microscopic level, DGL- α immunolabelling was only found in dendritic spines (s) receiving asymmetric synapses, but not in boutons (b) (C). Conversely, in the case of MGL-immunostaining, we found immunopositivity exclusively in the axon terminals (b), but not in the spines (s) (D). Scale, A-B, 20 μ m, C-D, 500nm

While ample evidence proves the role of CB₁ on glutamate release and synaptic strength in the neocortex (e.g. Domenici et al., 2006), previous anatomical studies failed to detect CB₁ on glutamatergic axon terminals of the primary somatosensory cortex (S1) (Bodor et al., 2005; Deshmukh et al., 2007). To assess the cellular and subcellular distribution of CB₁ in principal neurons of the primary somatosensory cortex, we first performed ISH against CB₁ mRNA. The stainings revealed the expression of the receptor in neocortical pyramidal cells, although at low levels compared to that of certain interneurons. The specificity of the staining has been verified using slices taken from CB₁ knockout animals (produced by Prof. Andreas Zimmer, University of Bonn). Next, we carried out immunostainings with a highly sensitive antibody (Fukudome et al., 2004) to unequivocally confirm that CB₁s are present on neocortical glutamatergic axon terminals (Fig. 5A-C). Double immunostaining against CB₁ and DGL- α has revealed that these two key molecules of endocannabinoid signaling are indeed

targeted pre- and postsynaptically, respectively, to the same synapses (Fig. 5D). Finally, we have elucidated the synapse type-selective localization of CB₁ utilizing double fluorescent immunostainings. While we could detect CB₁ immunoreactivity on VGlut1-positive intracortical terminals, and on large GAD65-positive boutons of GABAergic interneurons, we haven't found any sign of the presence of the receptor on VGlut2-positive thalamocortical terminals (Fig. 5E).

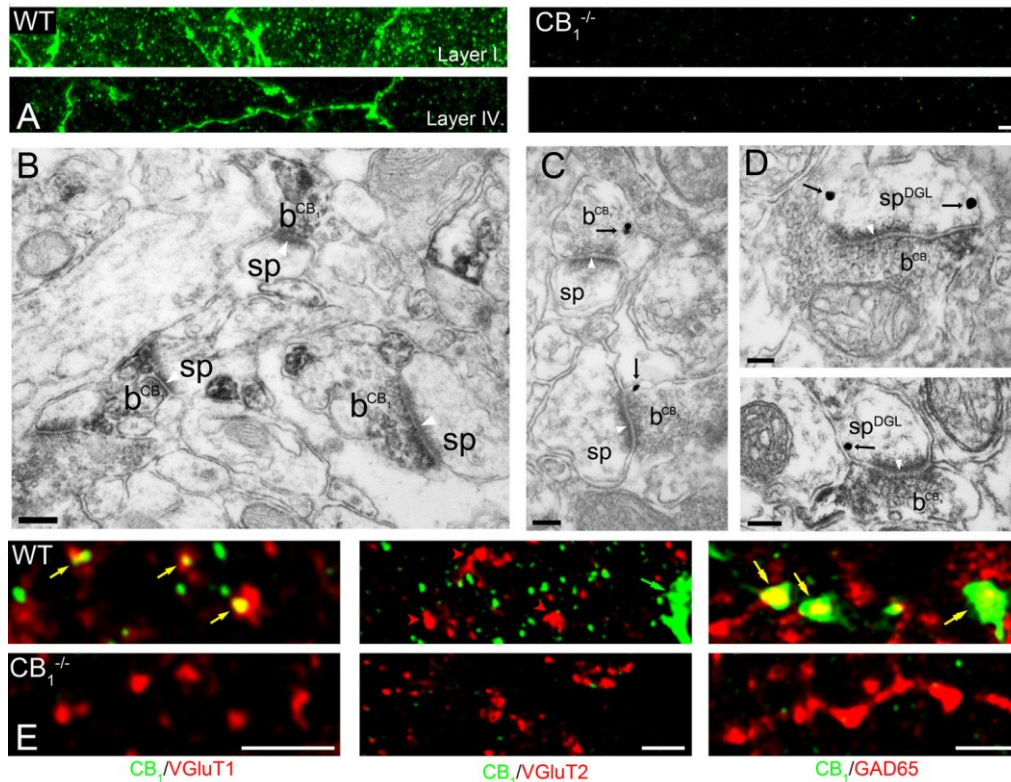


Figure 5. Localization of CB₁ receptor at neocortical synapses. (A) Immunofluorescence against CB₁ receptor in the somatosensory cortex of wild-type (WT) and CB₁ knockout (KO) littermates reveals specific labeling of fibers with large varicosities and small punctae, with a decreased density of the punctae in layer IV. (B) Electron micrographs of peroxidase-based staining indicate that the receptor is present in glutamatergic boutons (b), raising asymmetric synapses (white arrowheads) on dendritic spines (sp). (C) Immunogold labeling (arrows) reveals that CB₁ is targeted to the plasma membrane of axon terminals, near synapses. (D) Double staining against CB₁ (immunoperoxidase) and DGL- α (immunogold) shows that postsynaptic DGL- α and presynaptic CB₁ are present in the same synapses. (E) Double immunofluorescent staining against CB₁ and presynaptic markers of different pathways detected CB₁ receptor on intracortical (VGlut1-positive), but not on thalamocortical (VGlut2-positive) glutamatergic axon terminals, and high levels of the receptor on a subset of GABAergic (GAD65-positive) boutons. Scale bars: 2 μ m for (A) and (E), 200 nm for (B), and 100 nm for (C-D).

As there is no evidence of CB₁ receptors on thalamocortical axons or CB₁ expression in the sensory thalamic nuclei, and none of the known plasticity mechanisms of thalamocortical synapses involve eCBs, it is very likely that these axon terminals are devoid of cannabinoid receptors. Interestingly, we could clearly demonstrate the presence of DGL- α postsynaptically to thalamocortical boutons, identified either based on VGlut2 immunoreactivity or by anterograde tracer injections into the VPM (Figure 3G). Taken together, these results render the well-known homosynaptic modus operandi of eCB-mediated depression very unlikely at thalamocortical synapses, and raise the possibility of the presence of other, predominantly heterosynaptic eCB signaling mechanisms.

Objective 3

Although, unfortunately, we could not set up our own colony of DGL- α knockout mice, we have obtained brain samples from littermate wild type and DGL- α KO mice (described by Tanimura et al., 2010). To provide robust negative controls for our anatomical experiments, we carried out immunostainings, processing the WT and KO sections together throughout the procedure. Staining in the KO sections resulted in a very weak labeling of some sparsely scattered punctae (Fig. 3). According to our electron microscopical analysis, the majority of the residual

labeling in the KO was associated to dendritic mitochondria and microtubules, and to glial processes. In the wild type, 104 of 326 dendritic spines (~32%) contained the immunoreaction end product, while only 6 spines of 336 (~2%) did in the knockout. Thus, we could unequivocally verify the results we have achieved using the “DGL- α INT” antibody.

Objective 4

Confirmation of the specificity of ISH and ICH experiments for DGL- α are discussed above in Objective 1 and 3, respectively and demonstrated in Figure 1 and 2.

Objective 5

Input-dependent distribution of DGL- α was presented in Figure 3 and discussed under Objective 2.

Specific aim 2

Objective 6

We aimed to investigate the effect of mutations of DGL- α on the enzyme’s activity and localization in the excitatory synapses by the delivery of expression vector constructs into hippocampal primary neurons.

First, we generated two vector constructs expressing DGL- α enzyme fused with green fluorescent protein (GFP). Using pAcGFP-C and pAcGFP-N expression vectors, we generated GFP-DGL- α N-terminally tagged (Fig. 6A) and DGL- α -GFP C-terminally tagged (Fig. 6C) fusion constructs, respectively. Following cloning, we selected the bacterial colonies carrying the appropriate construct by restriction enzyme digestion of the mini-prep DNA solution (Fig. 6B,D), and proved the lack of mutations by sequencing.

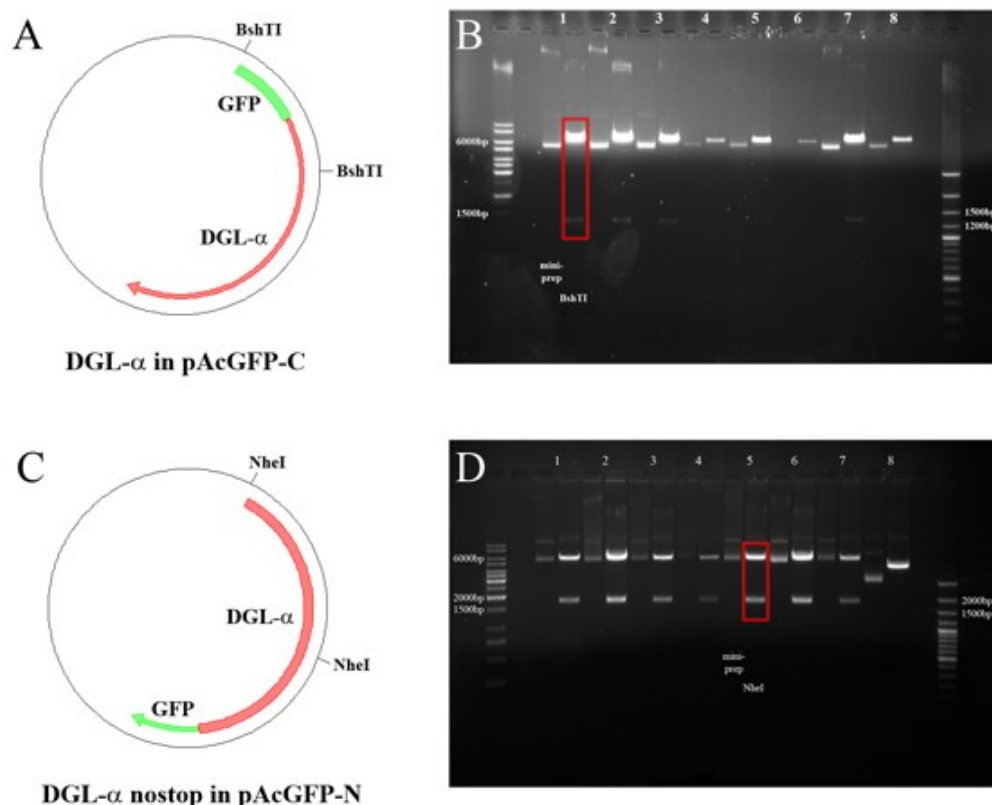


Figure 6. Plasmid constructs expressing DGL- α tagged with green fluorescent protein. (A), Vector construct expressing GFP-DGL- α fusion-protein. Recognition sites for BshTI restriction enzyme are labelled. (B), Gel-electrophoretic analysis of restriction enzyme digestion of mini-preps showed that BshTI digestion resulted in the desired 6600bp and 1300bp long DNA products for example in the case of clone 1. (C), Vector construct expressing DGL- α -GFP fusion-protein. Recognition sites for NheI restriction enzyme are labelled. (D), Gelelectrophoretic analysis of restriction enzyme digestion of mini-preps showed that NheI digestion resulted in the desired 6000bp and 1800bp long DNA products for example in the case of clone 5.

Objective 7

The DGL- α -GFP expression constructs were transfected into hippocampal primary neuronal cell culture using lipofectamine, and we examined whether the localization of the fluorescently labelled DGL- α is identical to the postsynaptic localization of native DGL- α . Light microscopic investigations revealed that the fluorescently labelled DGL- α is present in the dendrites of transfected hippocampal cells for both DGL- α -GFP and GFP-DGL- α constructs (Fig.7A-B). To prove the correct postsynaptic localization of DGL- α -GFP fusion protein, we performed fluorescent immunostaining for the presynaptic marker Bassoon. GFP fluorescence and Bassoon immunostained puncta did not overlap at high magnification, however they were in close apposition with each other suggesting that DGL- α -GFP protein is localized in dendritic spineheads (Fig. 7B). In forthcoming electron microscopic experiments, we will prepare ultrathin sections of the transfected cells to further investigate the subcellular targeting of the fluorescently tagged DGL- α in our model system.

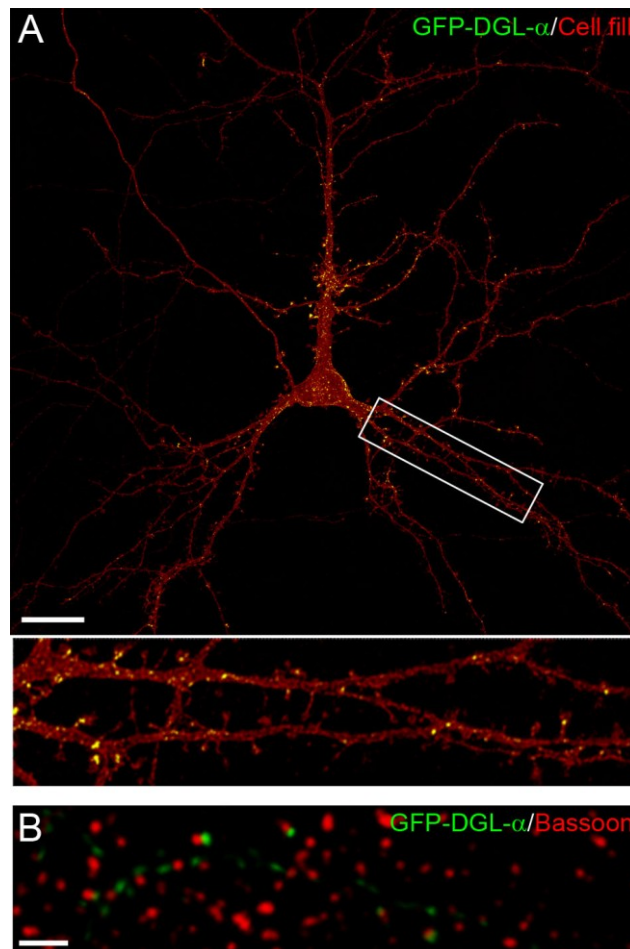


Figure 7. Spine localization of GFP-tagged DGL- α in cultured hippocampal neurons. (A), GFP-DGL- α signal is enriched in the somatic plasma membrane and dendritic spines of a DIV21 neuron. (B) In distal dendrites, DGL- α is concentrated into punctae contacting the presynaptic active zone marker Bassoon, indicating postsynaptic targeting of the construct. Scale bars: 10 μ m for (A), 5 μ m for (B).

Objective 8

In the proposed project plan, we aimed to investigate the role of DGL- α and DGL- β enzymes in mGluR-mediated synaptic plasticity using silencing RNAi constructs. We did not pursue this research direction further, because Tanimura and colleagues published a paper in *Neuron* in 2010 investigating the same question. They have generated DGL- α and DGL- β knockout mice to study the contribution of these enzymes to retrograde signaling. They have shown that the suppression of endocannabinoid-mediated retrograde signaling is impaired in the DGL- α knock-out mice, but is intact in DGL- β knock-out animals, so 2-AG synthesised by DGL- α is responsible for mediating the suppression of synaptic retrograde signaling.

Objective 9

Using an in silico search, we have identified serine residues of the C-terminal tail of DGL- α that are potentially available for phosphorylation, and thus might regulate the activity and localization of the DGL- α enzyme. These serine residues (S723, S730, S733, S804, S808) are evolutionarily conserved (Fig. 8, top), and are indeed phosphorylated according to proteomic analysis of synaptic preparations. To investigate the role of activity-dependent phosphorylation of DGL- α at these serine residues, we generated loss-of-function mutations of these selected serines to alanine. We used a site-directed mutagenesis technique to generate these constructs from fluorescently labelled DGL- α expression vectors. We optimized the method to achieve ~95% success rate for mutagenesis based on colour-dependent selection of transformed bacterial colonies, which was further verified by sequencing. Using the correct primers (Fig. 8, bottom), this rapid and reliable technique allows the preparation of loss-of-function mutants in the DGL- α -GFP fusion protein expressing vectors to investigate the effect of these mutations on the anatomical localization and physiological function of DGL- α in the subsequent experiments.

| | 723 | 730 | 733 | 804 | 808 |
|------------|--------------------|-------------------|-----|-----|-----|
| Human | S VRSKSQ EM LEGFSE | DSRRSSGFR IRG PSL | | | |
| Chimpanzee | S VRSKSQ EM LEGFSE | DSRRSSGFR IRG PSL | | | |
| Rhesus | EPVGSKSQ EM LEGFSE | DSRRSSGFR IRG PSL | | | |
| Rat | S VRSKSQ EM LEGFSE | DSRRSSGFR IRG PSL | | | |
| Mouse | S VRSKSQ EM LEGFSE | DSRRSSGFR IRG PSL | | | |
| Chicken | S TKSKSH EI LEGFYE | DSRRSSGFR IRG PSL | | | |
| Danio | S VRSCAR EI LDGFSE | DSRRSSA--ALRG PCL | | | |
| Pufferfish | S VRSCAQ EI LDGFSE | DSRRSSA--ALRG PML | | | |

S723A: AGT → GCT
forw S723A: AGAGCATCGCAACAGCGCTGT CAGGAGCAAGTC
rev S723A: GACTTGCTCCTGACAGCGCTGTTGCGATGCTCT

S730A: TCT → GCT
forw S730A: CAGGAGCAAGTCTCAGGCTGAGATGAGTCTGG
rev S730A: CCAGACTCATCTCAGCCTGAGACTTGCTCCTG

S733A: AGT → GCT
forw S733A: GTCTGAGATGGCTCTGGAGGGCTTCTCT
rev S733A: AGAGAAGCCCTCCAGAGCCATCTCAGAC

S804A: AGC → GCC
forw S804A: CTCCTCAGGCTTCCGAGCCATCAGAGGCTCGCCAG
rev S804A: CTGGGCGAGCCTCTGATGGCTCGGAAGCCTGAGGAG

S808A: TCG → GCG
forw S808A: CCGAAGCATCAGAGGCGCGCCAGCCTCCATGC
rev S808A: GCATGGAGGCTGGGCGCGCCTCTGATGCTTCGG

Figure 8. Top: Candidate phosphorylated serine (S) residues of DGL- α identified by in silico analysis of proteomic studies using synaptic preparations. Note that the serine residues that might be target for activity-dependent phosphorylation (highlighted in black) are evolutionarily conserved in phylogenetically distant species. Bottom: Primer sequences used for loss-of-function mutation of serine residues, mutated nucleotides are in red.

We also planned to address the role of a conserved Homer binding motif in DGL- α and the long isoforms of Homer in coupling DGL- α and mGluR in the perisynaptic signaling machinery. However, we finally did not perform these experiments, because the role of Homer in the regulation of DGL- α activity has been revealed by the group of Stephan Ikeda (Won et al, 2009). They have prepared a model system in isolated rat sympathetic neurons by sequential addition of molecular components to investigate the minimal molecular requirement for a functional endocannabinoid system. They identified mGluR5a, Homer 2b, DGL- α and CB₁ receptors as critical elements required to recapitulate retrograde endocannabinoid production and detection, thus confirming our original hypothesis.

Therefore we chose an alternative approach to study the regulation of DGL- α . We examined the role of DGL- α and mGlu $_5$ coupling in Fragile X syndrome (FXS). Fragile X syndrome is the most common form of inherited mental retardation and is caused by genetic silencing of the *fmr1* gene, resulting in loss of the fragile X mental retardation protein (FMRP). The “mGlu-Theory” of FXS states that enhanced group I metabotropic glutamate receptor (mGlu) activity may explain the phenotypic manifestation of FXS (Bear et al., 2004). Glutamatergic synapses in the nucleus accumbens express a form of long term depression (LTD) requiring endocannabinoid (eCB) production via activation of postsynaptic mGlu $_5$ receptors and their coupling to DGL- α (Robbe et al., 2003). Based on the “mGlu-theory”, we expected an enhancement of this form of synaptic plasticity at these synapses, however to our surprise; mGlu $_5$ -induced-LTD was completely absent in FMR1-/- mice (Figure 9A). Other synaptic properties were normal in both groups, basal eCB levels and CB $_1$ receptor function was unaltered (data not shown), however a significant decrease in mGlu $_5$ -induced DGL- α activity was observed in synaptoneurosomes prepared from FMR1-/- mice (Figure 9B), suggesting that FMRP loss resulted in a specific functional uncoupling of mGlu $_5$ from DGL- α . To test this hypothesis, we performed a detailed electron microscopy study, which revealed that DGL- α distribution was concentrated perisynaptically at glutamatergic synapses in wild type, but not in FMR1-/- mice (Figure 9C). Instead, DGL- α was distributed sporadically along the spine head membrane and often within the spine head cytoplasm in FMR1-/- animals. Interestingly, a similar biased perisynaptic distribution of mGlu $_5$ was found in both groups (Figure 9D), suggesting that DGL- α is specifically mis-targeted following FMRP knockout. Thus, we conclude that absence of FMRP results in loss of eCB-LTD in the nucleus accumbens, which may be explained by functional uncoupling of mGlu $_5$ and DGL- α at glutamatergic synapses.

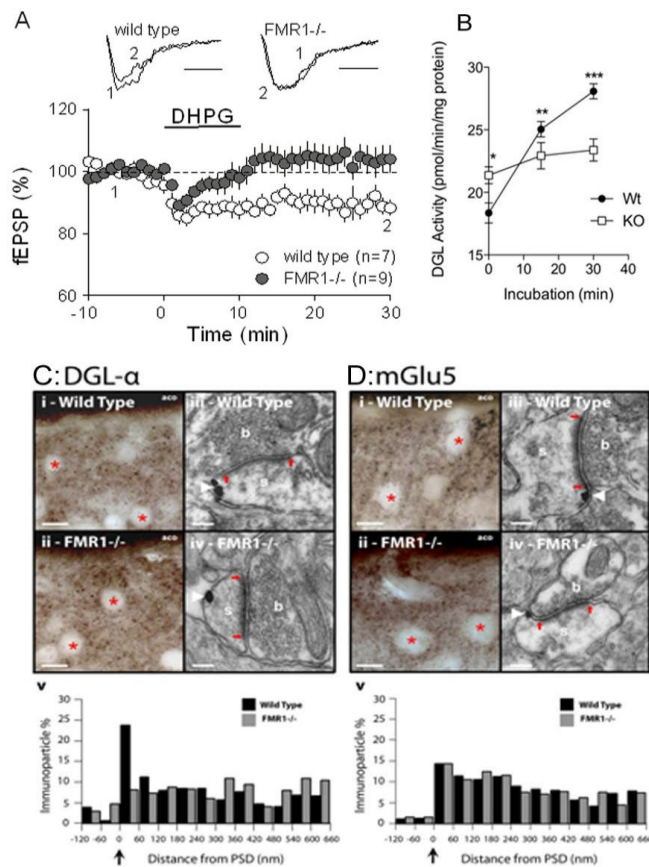


Figure 9. Fragmentation of the eCB system following FMRP knockout

(A) Activation of mGlu $_5$ with 50 μ M (S)-DHPG induces long term depression in wild type littermates (open circles) but not FMR1-/- mice (filled circles). Summary graph showing excitatory post synaptic field potentials (fEPSP) amplitudes. Values are normalized to baseline before the induction of LTD and averaged per minute.

(B) Synaptoneurosomes were prepared from whole brain of wild-type or FMR1-/- mice. The fractions (1 mg/ml) were incubated at 37 $^{\circ}$ C for the indicated time in the presence or absence of 100 μ M DHPG and DGL activity was measured (n=3).

(C) (i, ii) Light micrographs of DGL- α immunoperoxidase labeling in WT (i) and FMR1-/- mice (ii). The granular staining of DGL- α -immunoreactivity in the neuropil of the nucleus accumbens suggests a compartmentalized localization of the enzyme in WT and FMR1-/- mice. Medium spiny neuron somata are largely devoid of labeling (asterisks). aco – anterior commissure, s – spine head, b - bouton. (iii, iv) Electron micrographs of asymmetric synapses displaying DGL- α -immunogold labeling, in WT (iii) and FMR1-/- mice (iv). Gold particles representing the precise localization of DGL- α (arrowheads) are predominantly found in the perisynaptic domain close to the PSD (small arrows) in WT animals, whereas in synapses from FMR1-/- animals, gold particles are usually found in more distal locations from the PSD. (v) Histogram summarizing the skewed perisynaptic distribution of normalized

DGL- α -immunogold particles on the plasma membrane of dendritic spine heads in WT mice (black bars, n = 259), and the lack of biased distribution in FMR1-/- mice (grey bars, n = 185). Large arrowhead represents the edge of the PSD.

(D) (i, ii) Light micrographs of mGlu $_5$ immunoperoxidase labeling in WT (i) and FMR1-/- animals (ii). mGlu $_5$ -immunoreactivity displays a similar granular pattern of labeling as DGL- α , with medium spiny neuron somata largely devoid of labeling (asterisks). aco – anterior commissure, s – spine head, b - bouton. (iii, iv) Electron micrographs of asymmetric synapses displaying mGlu $_5$ -immunogold labeling (arrowhead), in WT (iii) and FMR1-/- animals (iv). In contrast to DGL- α localization, mGlu $_5$ was predominantly found in the perisynaptic domain adjacent to the PSD (red arrows) in both WT and FMR1-/- mice. (v) Histogram representing the similar normalized distribution of mGlu $_5$ -immunogold particles on dendritic spine heads in WT (black bars, n = 294) and FMR1-/- animals (grey bars, n = 285). Large arrowhead points to the edge of the PSD. Scale bars: 15 μ m in Ci, Cii, Di, Dii and 100 nm in Ciii, Civ, Diii, Div.

Specific aim 3

Diacylglycerol lipases generate monoacylglycerols by the cleavage of diacylglycerols. Two isoforms of this enzyme have been cloned (Bisogno et al., 2003), of which the α isoform has been identified as the synthetic enzyme of synaptic endocannabinoids (Katona et al., 2006; Tanimura et al., 2010). However, knockout of the second isoform, DGL- β , did not alter neither endocannabinoid-mediated synaptic plasticity, nor brain 2-AG levels (Tanimura et al., 2010). Thus, the function of this enzyme in the adult brain has remained elusive to date. To aid generation of hypotheses for the role of DGL- β , in our third specific aim, we have attempted to assess the expression pattern and subcellular localization of the enzyme. Our preliminary *in situ* hybridization and immunostaining results suggested that DGL- β is abundantly expressed by adult mouse hippocampus and cortex, and, at the protein level, the enzyme is targeted to the postsynaptic plasma membrane, near symmetric, putatively GABAergic synapses. While similar staining patterns with multiple antibodies raised against independent epitopes suggested the specificity of stainings, lack of access to DGL- β knockout animals prevented the rigorous verification of the results.

Objectives 1,2,3,4,5 and 8 (corresponding to DGL- β experiments)

To overcome the limitations of using antibodies, we have first generated EGFP-tagged DGL- β constructs to study the localization of the enzyme in cultured primary hippocampal neurons. We have successfully cloned the coding sequence of the DGL- β gene from cDNA reverse transcribed from total adult mouse hippocampal RNA, thus, in spite of the lack of knockout control for our ISH results, we could unequivocally prove DGL- β expression in the adult brain at the mRNA level. Transfection of cultured neurons with DGL- β tagged either on the N- or on the C-terminal revealed the somatodendritic targeting of the enzyme (Fig. 10). The signal was accumulated in discrete punctae in dendrites, both in shafts and spines. Our preliminary electron microscopic results of anti-EGFP immunogold stainings of cultured neurons suggest that surprisingly, unlike DGL- α , the β isoform is not targeted to the plasma membrane, but localized on intracellular membrane compartments. Using the constructs, we could directly test the sensitivity of our different antibodies on transfected neurons (Fig. 11). All of our antibodies detected overexpressed DGL- β , however, certain antibodies also stained somata of untransfected cells, questioning their specificity.

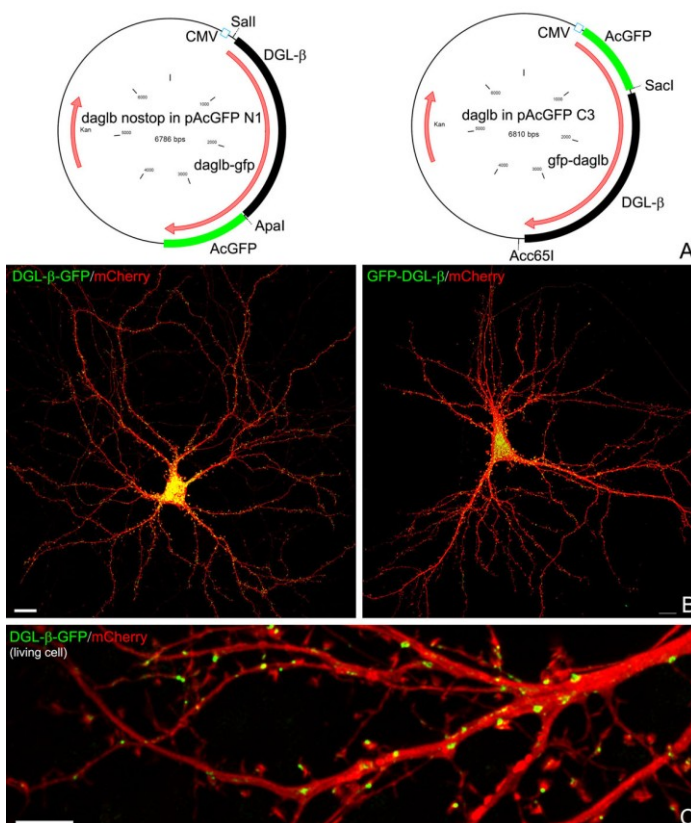


Figure 10. Generation of tagged DGL- β constructs (A) Maps of constructs of DGL- β tagged on the C- and N-terminal. (B) Confocal micrographs of DIV21 primary hippocampal neurons expressing either construct reveal somatodendritic localization of tagged DGL- β . (C) The tagged enzyme has accumulated in punctae inside dendritic shafts and spines. Scale bars: 10 μ m for (B), 5 μ m for (C).

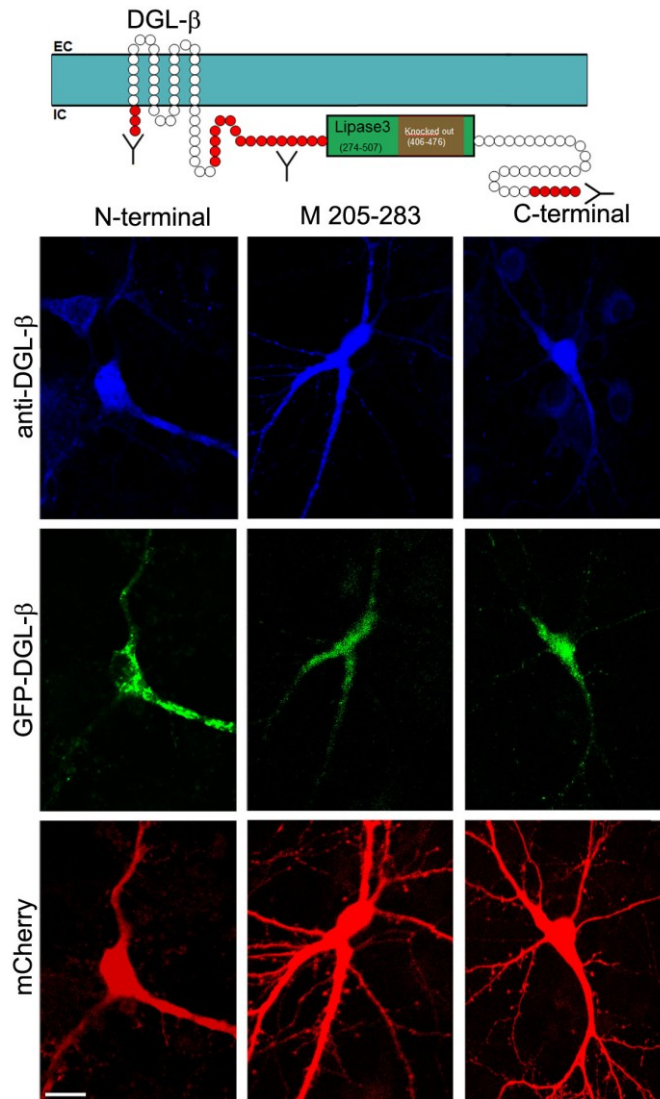


Figure 11. Schematic representation of DGL- β depicting the location of epitopes used to generate antibodies. The lipase3 motif, and the region targeted in the knockout by Kano et al. are also marked. We have verified the sensitivity of the antibodies utilizing cultured primary hippocampal neurons overexpressing DGL- β . Note the cytoplasmic immunoreactivity of untransfected cells using the C- and N-terminal antibodies. Scale bar: 10 μ m.

We have set up a collaboration with Prof. Andreas Zimmer to gain access to DGL- β knockout mice for the essential negative control experiments. Unfortunately, Prof. Zimmer could not accomplish the generation of the mice to date. However, while we could not set up our own breeding colony, we have received fixed brains of littermate wild type (WT) and DGL- β knockout (KO) mice from Prof. Masanobu Kano (described by Tanimura et al., 2010). Immunostainings resulted in the same intensity and pattern in WT and KO samples (Fig. 12), indicating very strong aspecific binding of all of our antibodies, rendering them useless for immunohistochemical applications.

Taken together, while, due to technical limitations, we could not accomplish our objectives as planned, using alternative methods, we could confirm the expression of DGL- β in the adult rodent hippocampus, and the somatodendritic localization of the enzyme in cultured hippocampal neurons. We are working on the generation of new antibodies and will continue the experiments in the forthcoming years.

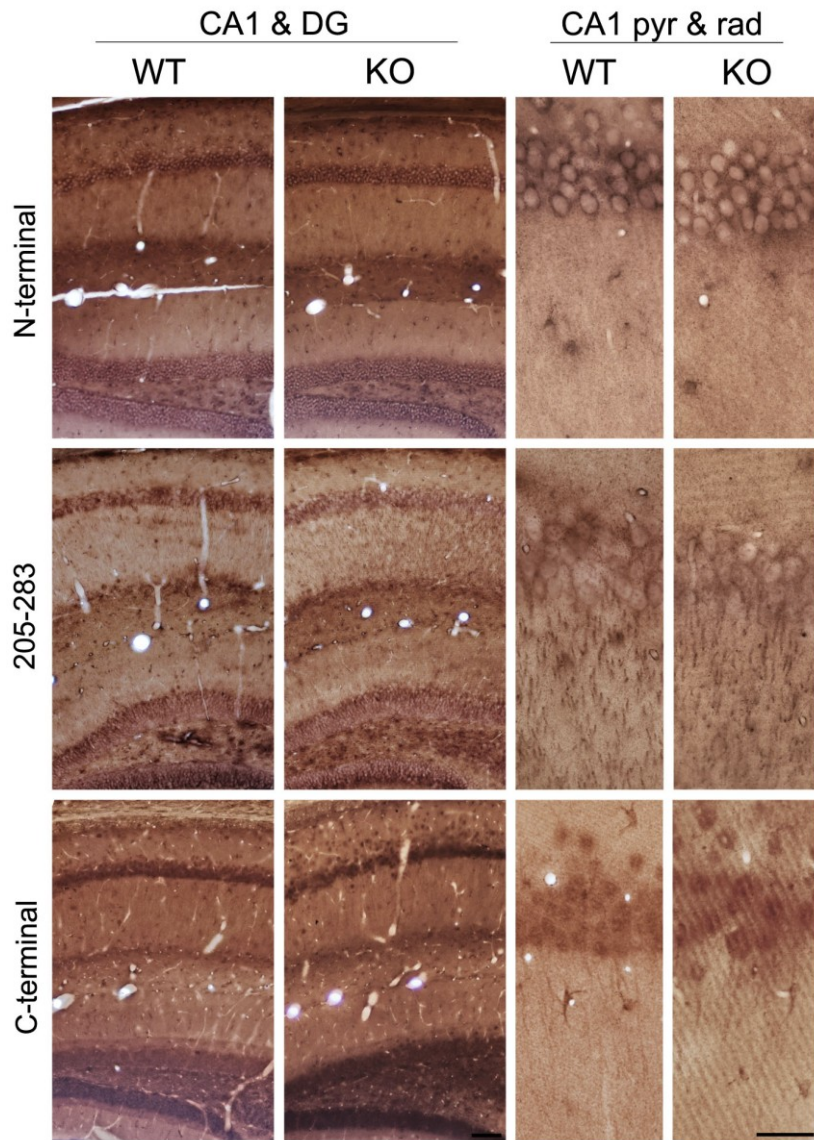


Figure 12. Immunostainings with antibodies raised against 3 independent epitopes has resulted in similar staining patterns in the hippocampus of wild-type (WT) and DGL- β knockout (KO) animals. Scale bars: 100 μ m/20 μ m.

References

- Birtoli B, Ulrich D (2004) Firing mode-dependent synaptic plasticity in rat neocortical pyramidal neurons. *J Neurosci* 24:4935-40
- Bisogno T, Howell F, Williams G, Minassi A, Cascio MG, Ligresti A, Matias I, Schiano-Moriello A, Paul P, Williams E, Gangadharan U, Hobbs C, Di Marzo V, Doherty P (2003) Cloning of the first sn1-DAG lipases points to the spatial and temporal regulation of endocannabinoid signaling in the brain. *J Cell Biol* 163:463-8
- Bodor AL, Katona I, Nyiri G, Mackie K, Ledent C, Hajos N, Freund TF (2005) Endocannabinoid Signaling in Rat Somatosensory Cortex: Laminar Differences and Involvement of Specific Interneuron Types. *J. Neurosci.* 25:6845-6856
- Chevalyere V, Takahashi KA, Castillo PE (2006) Endocannabinoid-mediated synaptic plasticity in the CNS. *Annu Rev Neurosci* 29:37-76
- Crozier RA, Wang Y, Liu C, Bear MF (2007) Deprivation-induced synaptic depression by distinct mechanisms in different layers of mouse visual cortex. *Proc Natl Acad Sci U S A* 104:1383-8

- Deshmukh S, Onozuka K, Bender KJ, Bender VA, Lutz B, Mackie K, Feldman DE (2007) Postnatal development of cannabinoid receptor type 1 expression in rodent somatosensory cortex. *Neuroscience* 145:279-87
- Domenici MR, Azad SC, Marsicano G, Schierloh A, Wotjak CT, Dodt H, Zieglgänsberger W, Lutz B, Rammes G (2006) Cannabinoid receptor type 1 located on presynaptic terminals of principal neurons in the forebrain controls glutamatergic synaptic transmission. *J Neurosci* 26:5794-9
- Fukudome Y, Ohno-Shosaku T, Matsui M, Omori Y, Fukaya M, Tsubokawa H, Taketo MM, Watanabe M, Manabe T, Kano M (2004) Two distinct classes of muscarinic action on hippocampal inhibitory synapses: M2-mediated direct suppression and M1/M3-mediated indirect suppression through endocannabinoid signalling. *Eur J Neurosci* 19:2682-92
- Hannan AJ, Blakemore C, Katsnelson A, Vitalis T, Huber KM, Bear M, Roder J, Kim D, Shin HS, Kind PC (2001) PLC-beta1, activated via mGluRs, mediates activity-dependent differentiation in cerebral cortex. *Nat Neurosci* 4:282-8
- Katona I, Freund T (2008) Endocannabinoid signaling as a synaptic circuit breaker in neurological disease. *Nat Med* 14:923-30
- Katona I, Urbán GM, Wallace M, Ledent C, Jung K, Piomelli D, Mackie K, Freund TF (2006) Molecular composition of the endocannabinoid system at glutamatergic synapses. *J Neurosci* 26:5628-37
- Nevian T, Sakmann B (2006) Spine Ca²⁺ signaling in spike-timing-dependent plasticity. *J Neurosci* 26:11001-13
- Pacher P, Bátkai S, Kunos G (2006) The endocannabinoid system as an emerging target of pharmacotherapy. *Pharmacol Rev* 58:389-462
- Robbe D, Alonso G, Manzoni OJ (2003) Exogenous and endogenous cannabinoids control synaptic transmission in mice nucleus accumbens. *Ann N Y Acad Sci.* 1003:212-25
- Tanimura A, Yamazaki M, Hashimotodani Y, Uchigashima M, Kawata S, Abe M, Kita Y, Hashimoto K, Shimizu T, Watanabe M, Sakimura K, Kano M (2010) The endocannabinoid 2-arachidonoylglycerol produced by diacylglycerol lipase alpha mediates retrograde suppression of synaptic transmission. *Neuron* 65:320-327
- Wijetunge LS, Till SM, Gillingwater TH, Ingham CA, Kind PC (2008) mGluR5 Regulates Glutamate-Dependent Development of the Mouse Somatosensory Cortex. *J. Neurosci.* 28:13028-13037
- Won YJ, Puhl HL 3rd, Ikeda SR (2009) Molecular reconstruction of mGluR5a-mediated endocannabinoid signaling cascade in single rat sympathetic neurons. *J Neurosci.* 29(43):13603-12